

# Being heterogeneous is disadvantageous: Brownian non-Gaussian searches

Vittoria Sposini,<sup>1,\*</sup> Sankaran Nampoothiri,<sup>2,†</sup> Aleksei Chechkin,<sup>3,4,5,‡</sup>  
Enzo Orlandini,<sup>6,§</sup> Flavio Seno,<sup>6,¶</sup> and Fulvio Baldovin<sup>6,\*\*</sup>

<sup>1</sup>*Faculty of Physics, University of Vienna, Kolingasse 14-16, 1090 Vienna, Austria*

<sup>2</sup>*Department of Physics, Gandhi Institute of Technology and Management (GITAM) University, Bengaluru-561203, India*

<sup>3</sup>*Faculty of Pure and Applied Mathematics, Hugo Steinhaus Center,*

*Wroclaw University of Science and Technology, Wyspianskiego Str. 27, 50-370 Wroclaw, Poland*

<sup>4</sup>*Institute for Physics & Astronomy, University of Potsdam, 14476 Potsdam-Golm, Germany*

<sup>5</sup>*Akhiezer Institute for Theoretical Physics, 61108 Kharkov, Ukraine*

<sup>6</sup>*Dipartimento di Fisica e Astronomia ‘G. Galilei’ - DFA, Sezione INFN,  
Università di Padova, Via Marzolo 8, 35131 Padova (PD), Italy*

(Dated: March 18, 2024)

Diffusing diffusivity models, polymers in the grand canonical ensemble and polydisperse, and continuous time random walks, all exhibit stages of non-Gaussian diffusion. Is non-Gaussian targeting more efficient than Gaussian? We address this question, central to, e.g., diffusion-limited reactions and some biological processes, through a general approach that makes use of Jensen’s inequality and that encompasses all these systems. In terms of customary mean first passage time, we show that Gaussian searches are more effective than non-Gaussian ones. A companion paper argues that non-Gaussianity becomes instead highly more efficient in applications where only a small fraction of tracers is required to reach the target.

## INTRODUCTION

The Brownian non-Gaussian motion refers to the interesting contingency of observing a stochastic process characterized by a mean squared displacement which linearly increases in time – Brownian or Fickian behavior – concomitant with a non-Gaussian probability density function (PDF) for the displacements. Since its discovery in a variety of experimental conditions [1–18] and molecular dynamics simulations [19–21] it was expected [2] that the excess of probability for rare fluctuations might dominate first-passage processes. Recent analyses showed however that typical Gaussian searches turn out to be more effective than non-Gaussian ones [22–24]. This issue finds here a general assessment encompassing different experimental situations and theoretical models, including diffusing diffusivities [25], polymers in the grand canonical ensemble [26–28] and polydisperse [29–31], and continuous time random walks [32–36]. By using the Jensen’s inequality [37] we first show that the “tail effect” – associated with faster diffusion – is in fact accompanied by a “central effect”, i.e., an excess probability for slower diffusion. The question then comes up about which one is dominant in first-passage processes. The answer depends on the threshold for the fraction of tracers reaching the target which is relevant to the specific application. A further implementation of Jensen’s inequality allows us to demonstrate that indeed the typical time scale for one searcher to reach the target, e.g. the mean first passage time is shorter in Gaussian than in non-Gaussian diffusion. However, the scenario drastically changes if the relevant physical time scale is instead related to the first few successful searches among many: In this case, a companion paper [38] shows that the non-Gaussian behavior

becomes significantly faster than the Gaussian one.

In the next Section, we introduce the general mechanism leading to non-Gaussianity in subordination processes, highlighting the “tail” and “central” effects. After presenting various subordination models, we then proceed to highlight two dynamical regimes, characterized by different scaling properties of the PDF for the subordinator. Paradigmatic targeting problems are then discussed within this context, and we finally draw our conclusions.

## FASTER AND SLOWER DIFFUSION

Let us first recall how Brownian non-Gaussian diffusion emerges in subordination processes. Consider a situation in which some source of heterogeneity makes the diffusion coefficient  $D$  of overdamped particles to fluctuate in time (examples are provided below). Indicating as  $X(t)$  the random location along a certain axis  $x$  at time  $t$  of the diffusing particle, we have

$$dX(t) = \sqrt{2D(t)} dB(dt), \quad (1)$$

where  $B(t)$  is a Wiener process (Brownian motion), and  $D(t)$  describes the stochastic process associated with the fluctuating diffusion coefficient. We indicate as  $p_D^*$  the steady-state distribution density of  $D(t)$ , which could either be a PDF or a probability mass function (PMF) depending on whether  $D$  varies continuously or discretely, and as  $D_{\text{av}} \equiv \mathbb{E}[D]$  its average value. Technically, it is convenient to introduce the *subordinator* process, defined as

$$S(t) \equiv 2 \int_0^t dt' D(t') \Rightarrow dS = 2 D(t) dt; \quad (2)$$

in such a way Eq. (1) is reexpressed in the *random path* or *subordinator parametrization* [25–28]:

$$dX(t) = dB(dS). \quad (3)$$

The PDF for the tracer in position  $x$  at time  $t$ , given that it was at  $x_0$  at time zero is then obtained through the subordination formula [39, 40]

$$p_X(x, t|x_0) = \int_0^\infty ds G_{\text{BG}}(x, s|x_0) p_S(s, t), \quad (4)$$

where  $p_S(s, t)$  is the probability for the path parametrization  $s$  at time  $t$ , and  $G_{\text{BG}}(x, s|x_0)$  is the Green function for the Brownian-Gaussian (BG) ordinary diffusion associated with the problem's boundary conditions.

It is remarkable that, given the common subordination structure, quite different stochastic models share the same qualitative non-Gaussian features; to introduce these features, let us first concentrate on free diffusion. In free diffusion (with natural boundary conditions),

$$G_{\text{BG}}(x, s|x_0) = \frac{e^{-\frac{(x-x_0)^2}{2s}}}{\sqrt{2\pi s}}, \quad (5)$$

and Eq. (4) already highlights the non-Gaussian nature of the diffusion, as the tracer's PDF is a superposition of Gaussian PDFs. A change of variable in Eq. (4) shows how the moments of  $X(t)$  are linked to those of the subordinator:

$$\mathbb{E}[(X(t)-x_0)^m] = G_{\text{BG}}^{(m)} \int_0^\infty ds p_S(s, t) s^{\frac{m}{2}} = G_{\text{BG}}^{(m)} \mathbb{E}[S^{\frac{m}{2}}(t)], \quad (6)$$

where

$$G_{\text{BG}}^{(m)} \equiv \int_{-\infty}^{+\infty} dx \frac{e^{-\frac{(x-x_0)^2}{2s}}}{\sqrt{2\pi}} (x-x_0)^m. \quad (7)$$

In this paper, we focus on equilibrium initial conditions for  $D(t)$ , i.e. we assume that  $D(t)$  is distributed according to the steady-state distribution  $p_D^*$  so that

$$\mathbb{E}[D(t)] = D_{\text{av}}. \quad (8)$$

Through Eq. (6) with  $m = 2$  and Eq. (2), this is sufficient to guarantee the Brownian behavior:

$$\mathbb{E}[(X(t) - x_0)^2] = \mathbb{E}[S(t)] = 2D_{\text{av}} t. \quad (9)$$

While Gaussian variables have zero excess kurtosis  $\kappa_X(t) - 3$ , with the kurtosis defined as

$$\kappa_X(t) \equiv \frac{\mathbb{E}[(X(t) - x_0)^4]}{(\mathbb{E}[(X(t) - x_0)^2])^2}, \quad (10)$$

subordination processes are leptokurtic, that is, they are characterized by a positive excess kurtosis. This is again

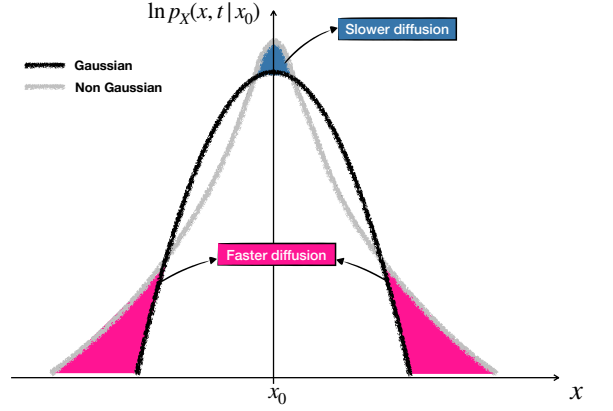


Figure 1. Comparison between Gaussian and non-Gaussian PDFs for subordination processes. The two PDFs share the same mean and standard deviation but the non-Gaussian one has an excess probability both in the tails and in the center part. The non-Gaussian PDF is obtained from the FSP model with  $p = 0.99$  (See text).

a consequence of Eq. (6): Since  $G_{\text{BG}}^{(4)}/(G_{\text{BG}}^{(2)})^2 = 3$ , we have

$$\kappa_X(t) - 3 = 3 \frac{\mathbb{E}[S^2(t)] - (\mathbb{E}[S(t)])^2}{(\mathbb{E}[S(t)])^2} > 0. \quad (11)$$

As a result, subordination processes possess an *excess of probability in the tails* of the PDF, compared to a Gaussian PDF with equal variance (see Fig. 1). This effect is triggered by the faster diffusers in  $p_D^*$ .

On the other hand the Jensen's inequality [37] says that for a real-valued  $\mu$ -measurable function  $f$  on a sample space  $\Omega$  and a convex function  $\varphi$  on the real numbers we have

$$\int_{\Omega} d\mu (\varphi \circ f) \geq \varphi \left( \int_{\Omega} d\mu f \right), \quad (12)$$

where the “ $\circ$ ” symbol means a composition of the functions. The inequality becomes strict if  $\varphi$  is strictly convex and the measure  $\mu$  is not induced by a constant random variable. Note now that  $\varphi(s) \equiv G_{\text{BG}}(x_0, s|x_0) = 1/\sqrt{2\pi s}$  is a convex function of  $s$ . Taking  $d\mu \equiv ds p_S(s, t)$  and  $f(s) \equiv s$ , we thus have that for all time  $t$ ,

$$\begin{aligned} p_X(x_0, t|x_0) &= \int_0^\infty ds p_S(s, t) G_{\text{BG}}(x_0, s|x_0) \\ &> G_{\text{BG}} \left( x_0, \int_0^\infty ds p_S(s, t) s \middle| x_0 \right) \\ &= G_{\text{BG}}(x_0, \mathbb{E}[S(t)]|x_0). \end{aligned} \quad (13)$$

Since both  $p_X(x, t|x_0)$  and  $G_{\text{BG}}(x, s|x_0)$  are continuous around  $x_0$ , there must exist a neighborhood of the center  $x_0$  in which this inequality remains valid. Thus, the non-Gaussian PDF also has an *excess of probability in the central part* compared to the Gaussian PDF, due to

slower tracers (again, please refer to Fig. 1). The natural question to address is which of these effects is dominant when considering targeting processes.

## SUBORDINATION STOCHASTIC MODELS

The subordination class includes a variety of stochastic models, depending on the details of the subordinator:

- (i) Diffusing diffusivity (DD) models [25] are obtained assuming the diffusion coefficient to be the square of an Ornstein-Uhlenbeck process,  $D(t) \equiv \mathbf{Y}^2(t)$ , with

$$d\mathbf{Y}(t) = -\frac{\mathbf{Y}(t)}{\tau} dt + \sigma d\mathbf{B}_{\mathbf{Y}}(dt). \quad (14)$$

The dimension of the vector  $\mathbf{Y}(t)$  is  $d_{\mathbf{Y}} \in \mathbb{N}^*$ ,  $\tau$  is the autocorrelation of the process, and  $\sigma$  defines the intensity of the fluctuations. The steady-state PDF is given by

$$p_D^*(D) = \frac{D^{d_{\mathbf{Y}}/2-1} e^{-d_{\mathbf{Y}} D/(2D_{\text{av}})}}{(2D_{\text{av}}/d_{\mathbf{Y}})^{d_{\mathbf{Y}}/2} \Gamma(d_{\mathbf{Y}}/2)}, \quad (15)$$

where  $D_{\text{av}} = \sigma^2 \tau d_{\mathbf{Y}}/2$  is the average diffusion coefficient. Under the name of “stochastic volatility”, these models are used in finance to correct the Black-Scholes option pricing for non-Gaussian effects [41, 42].

Simulation of the DD model can be simply realized by updating in parallel two Ornstein-Uhlenbeck processes: The one for  $\mathbf{Y}(t)$  and the one for  $X(t)$ . In the latter, at each update the increment is drawn from a normal distribution with zero average and variance  $2D(t) = 2\mathbf{Y}^2(t)$ . The simulation time can be expressed in terms of  $\tau$  and the other two free parameters are  $\sigma$  and  $d_{\mathbf{Y}}$ .

- (ii) A concrete simple example of a subordination process is offered by a polymer in a diluted solution, exchanging monomers with a chemostat: the Grand canonical polymer (GCP) model [26–28]. Indeed, the center of mass of a polymer in solution is known to diffuse with a coefficient  $D$  which depends on the number of monomers  $N$  as  $D(N) = D_1/N^\alpha$  [43, 44], with  $D_1$  the diffusion coefficient of a single monomer. The value of  $\alpha$  depends on the specific polymer model; for definiteness in this paper we adopt the Rouse value  $\alpha = 1$ , but similar results apply to other models, such as the Zimm or the reptation ones [44]. In the grand canonical ensemble  $N$  fluctuates in time, becoming a second source of noise besides the solvent collisions responsible for the Brownian motion.  $N(t)$  can be simply modeled in terms of a birth-death process; in the mean-field limit, both the birth  $\lambda$

and death  $\mu$  reaction rates are independent of the polymer size and their ratio  $p \equiv \lambda/\mu$  corresponds to the ratio between the fugacity of the system and the critical fugacity [27]: As  $p \rightarrow 1^-$ , the average polymer size becomes infinite and relative size fluctuations diverge. The steady-state size distribution is

$$p_N^*(n) = (1-p)p^{n-1} \quad \text{for } n = 1, 2, \dots, \quad (16)$$

corresponding to the diffusion coefficient PMF

$$p_D^*(D_n) = (1-p)p^{D_1/D_n-1}, \quad (17)$$

with  $D_n = D_1/n$ .

Also for the GCP model simulations are realized through a parallel update, in this case of the processes  $N(t)$  and  $X(t)$ . A simple way to simulate the birth-death process  $N(t)$  is by implementing the Gillespie algorithm [45] with reaction rates  $\lambda$ ,  $\mu$ . As reported for instance in Ref. [27], it is possible to approximate the autocorrelation time  $\tau$  of  $N(t)$  as

$$\tau = \frac{1+p}{(1-p)^2 \mu}, \quad (18)$$

where  $p = \lambda/\mu$ . It is clear from Eq. (18) that  $\tau$  diverges as  $p \rightarrow 1^-$ , a phenomenon called *critical slowing down*. While the ratio  $p = \lambda/\mu$  fixes the steady-state distribution  $p_N^*$  and how close the simulation is to critical conditions, the parameter  $\mu$  can still independently be fixed to calibrate the simulation time in terms of  $\tau$ , according to Eq. (18). The remaining free parameter is the single-monomer diffusion coefficient  $D_1$ .

- (iii) After polymerization terminates in a step-growth polymerization [31], one is left with a polydisperse sample of polymers with heterogeneous size  $N$ . Assuming chains with one reaction center in the end, the size distribution coincides with Eq. (16) and it is called in this context Flory-Schulz distribution [31], with  $p$  the *reaction extent*. In this case,  $D$  must be regarded as a static random variable,  $D(t) = D \forall t$ , distributed according to Eq. (17).

To simulate the behavior of the Flory-Schulz polydisperse (FSP) model, for each realization one simply picks a value of  $D_n$  with probability  $p_D^*(D_n)$ , and simulate then the Langevin process  $X(t)$  keeping the diffusion coefficient fixed. The statistic of the process is then obtained by averaging over the different histories. Free parameters are  $p$  and  $D_1$ .

- (iv) In the continuous time random walk (CTRW) [32–34, 36] with average waiting time  $\tau < \infty$ , one starts with a discrete subordinator  $K(t)$ , with  $p_K(k, t)$

the PMF for  $K = k \in \mathbb{N}$  steps operated at time  $t$ . If  $X(k)$  is a simple random walk providing the location after  $k$  steps with PDF  $p_{X_k}(x, k|x_0)$ , then one gets a discrete analogous of Eq. (4):

$$p_X(x, t|x_0) = \sum_{k=0}^{\infty} p_{X_k}(x, k|x_0) p_K(k, t). \quad (19)$$

For time  $t \gg \tau$  the typical number of steps is very large, and the operational time  $S(t)_{t \gg \tau} \equiv K(t)$  can be taken to be continuous, so that  $p_S(s, t)$  represents the probability for the continuous number of steps  $s$  operated at time  $t$ . Correspondingly, a typical random walk  $X(k)$  with finite variance tends to the Gaussian limit, recovering the subordination equation in the continuous form, Eq. (4).

Simulation of a CTRW simply proceeds as an ordinary random walk, once the value of the elapsed time taken by the update step is drawn from the assumed waiting-time distribution. Free parameters in the simulations are those defining the waiting-time distribution, in particular its average value  $\tau$ , and the length  $L$  of the random-walk step.

All these examples share the qualitative non-Gaussian features reported in Fig. 1.

## ASYMPTOTIC REGIMES

Before addressing search processes, some details about the dynamics are needed. Subordination processes may display two different regimes during which the PDF  $p_S(s, t)$  can be approximated in different ways. According to Eq. (11), the excess kurtosis evolves differently during the two regimes.

- *Super-statistics (SS) regime.* Consider a situation in which the diffusion coefficient is almost static,  $D(t) \simeq D \forall t$ , distributed according to  $p_D^*$ . This approximation is exact for the FSP model, case (iii) above, but it is also valid for cases (i) and (ii) taking a heterogeneous sample of tracers initially characterized by the distribution  $p_D^*$ , as long as we consider time  $t \ll \tau$ . Indeed, for times much smaller than the autocorrelation time each tracer in the DD and GCP models basically retains its initial diffusion coefficient. Within this approximation we have

$$S(t) = 2Dt, \quad (20)$$

and a change of variable yields

$$p_S(s, t) = \frac{1}{2t} p_D^*\left(\frac{s}{2t}\right). \quad (21)$$

From Eq. (11), the excess kurtosis is

$$\begin{aligned} \kappa_X(t) - 3 &= 3 \frac{\mathbb{E}[D^2] - (\mathbb{E}[D])^2}{(\mathbb{E}[D])^2} \\ &= \text{const.} > 0 \quad (\text{SS regime}). \end{aligned} \quad (22)$$

The SS regime is thus non-Gaussian; the behavior of the tracers can be characterized by operating an average of  $D$ -dependent quantities, over  $p_D^*$ . This “superposition of statistics” has been named in the literature super-statistics [2, 17, 46, 47], explaining the origin of the name.

- *Large deviation (LD) regime.* With  $t \gg \tau$  the subordinators of the DD and GCP models inherit from the Markovian evolution of  $D(t)$  a LD principle [48]:

$$p_S(s, t) \asymp e^{-tI_S(s/t)}. \quad (23)$$

Here, “ $\asymp$ ” stands for “the dominant part as  $t \rightarrow \infty$ ”, and  $I_S$  is a rate function. Eq. (23) implies a time evolution of the kurtosis  $\kappa_X(t)$  different from the previous one. The *cumulant generating function* of  $S(t)$  is defined as

$$\begin{aligned} K_S(k, t) &\equiv \ln \mathbb{E} \left[ e^{kS(t)} \right] \\ &= \sum_{m=1}^{\infty} \frac{K_S^{(m)}(t)}{m!} k^m, \end{aligned} \quad (24)$$

where  $K_S^{(m)}(t)$  is the cumulant of order  $m$  of  $S(t)$ . Using Eq. (23) and the Laplace method one has

$$K_S(k, t) = t \lambda_{S/t}(k), \quad (25)$$

with the *scaled* cumulant generating function [48] of  $S(t)/t$ ,  $\lambda_{S/t}$ , being time-independent. This means that within the LD approximation all the cumulants of  $S(t)$  scale linearly with time,  $K_S^{(m)}(t) \propto t$ . As a consequence, from Eq. (11) we obtain

$$\kappa_X(t) - 3 = \frac{K_S^{(2)}(t)}{(K_S^{(1)}(t))^2} \propto 1/t \quad (\text{LD regime}). \quad (26)$$

Within this regime, the central part of  $p_X(x, t)$  becomes Gaussian (central limit theorem [48]). As time passes by, the non-Gaussian behavior is relegated to larger and larger (lesser and lesser probable) fluctuations. The probability of the scaled subordinator  $S(t)/t$  concentrates around its average value, and (apart from large deviations) the typical behavior is a BG diffusion with coefficient  $D_{\text{av}}$ . Besides characterizing the DD and GCP models as  $t \gg \tau$  [25–28], one can directly calculate the CTRW, with an exponential waiting time distribution satisfies a LD principle [36] and Eq. (26) (namely,  $\kappa_X(t) - 3 = 3\tau/t$ ), for all time  $t \geq 0$ .

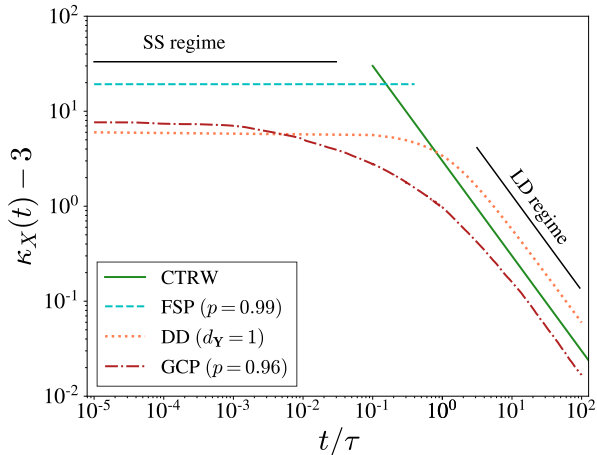


Figure 2. Time dependence of the excess kurtosis. A constant, positive  $\kappa_X - 3$  characterizes the SS regime, whereas in the LD regime  $\kappa_X(t) - 3 \sim 1/t$  (black solid lines). While for the GCP, DD, and CTRW models the excess kurtosis is reported as a function of the rescaled time  $t/\tau$ , for the FSP model it is plotted vs  $t$ . With these arrangements, the excess kurtosis depends only on the parameters displayed in the legend. Curves for the DD and the GCP models have been obtained simulating the models as described in the text; those for the FSP model and the CTRW with exponential waiting-time distribution have been exactly calculated.

Fig. 2 displays the time evolution of the excess kurtosis for the different models, highlighting the two regimes.

## NON-GAUSSIAN AND GAUSSIAN TARGETING

Let us now consider two classic targeting problems in one dimension:

- Finite interval  $[0, L]$  with absorbing boundaries at the extrema.
- Semi-infinite domain  $[0, \infty[$  with absorbing boundary at  $x = 0$ .

For ordinary diffusion, exact expressions [49] are available for the (cumulative) probability of reaching a target by time  $t$ , given the initial position  $x_0$  and the diffusion coefficient  $D$ ,

$$P_T(t|x_0, D) = 1 - \mathcal{S}_T(t|x_0, D) = 1 - \int dx G_{\text{BG}}(x, t|x_0, D) \quad (27)$$

( $\mathcal{S}_T$  is the survival probability):

- For the finite interval,

$$G_{\text{BG}}(x, t|x_0, D) = \frac{2}{L} \sum_{k=1}^{\infty} \sin\left(\frac{k\pi}{L} x\right) \sin\left(\frac{k\pi}{L} x_0\right) \cdot e^{-\left(\frac{k\pi}{L}\right)^2 D t}, \quad (28)$$

implying

$$P_T(t|x_0, D) = 1 - \frac{4}{\pi} \sum_{k=0}^{\infty} \sin\left(\frac{k\pi}{L} x_0\right) \frac{e^{-\left(\frac{k\pi}{L}\right)^2 D t}}{2k+1}. \quad (29)$$

- For the semi-infinite domain,

$$G_{\text{BG}}(x, t|x_0, D) = \frac{1}{\sqrt{4\pi D t}} \left[ e^{-\frac{(x-x_0)^2}{4 D t}} - e^{-\frac{(x+x_0)^2}{4 D t}} \right], \quad (30)$$

yielding

$$P_T(t|x_0, D) = 1 - \text{erf}\left(\frac{x_0}{\sqrt{4 D t}}\right). \quad (31)$$

The time derivative of these expressions provides the PDF for reaching the boundary at time  $t$ ,  $p_T(t|x_0, D) = \partial_t P_T(t|x_0, D)$ , from which one can obtain the characteristic time for a single particle to reach the target,  $\tau_T$ :

- With the finite domain,  $\tau_T$  is naturally given by the mean first passage time,

$$\begin{aligned} \tau_T(x_0, D) &= \int_0^{\infty} dt t p_T(t|x_0, D) \\ &= \frac{x_0(L-x_0)}{2D}. \end{aligned} \quad (32)$$

- The mean first passage time of the semi-infinite domain is infinite; however, a characteristic time can still be identified as [49]

$$\begin{aligned} \tau_T(x_0, D) &= \left[ \int_0^{\infty} dt t^\beta p_T(t|x_0, D) \right]^{1/\beta} \\ &= \frac{[\Gamma(1/2 - \beta)]^{1/\beta} x_0^2}{4 \pi^{1/(2\beta)} D}, \end{aligned} \quad (33)$$

for  $\beta < 1/2$ .

Given the two dynamical regimes discussed above, it is meaningful to contemplate the probability associated with the SS regime,

$$P_T^{\text{SS}}(t|x_0) \equiv \int_0^{\infty} dD p_D^*(D) P_T(t|x_0, D) \quad (34)$$

$$\equiv \sum_{n=0}^{\infty} p_D^*(D_n) P_T(t|x_0, D_n), \quad (35)$$

and the one corresponding to the LD regime,

$$P_T^{\text{LD}}(t|x_0) \equiv P_T(t|x_0, D_{\text{av}}). \quad (36)$$

According to Fig. 2 the behavior of the FSP model is characterized by the probability  $P_T^{\text{SS}}$  while the CTRWs for  $t \gg \tau$  are ruled by  $P_T^{\text{LD}}$ . For the DD model and the GCPs the actual probability will be close to  $P_T^{\text{SS}}$  for  $t \ll \tau$  and will tend to  $P_T^{\text{LD}}$  as  $t \gg \tau$ . In Fig. 3 we

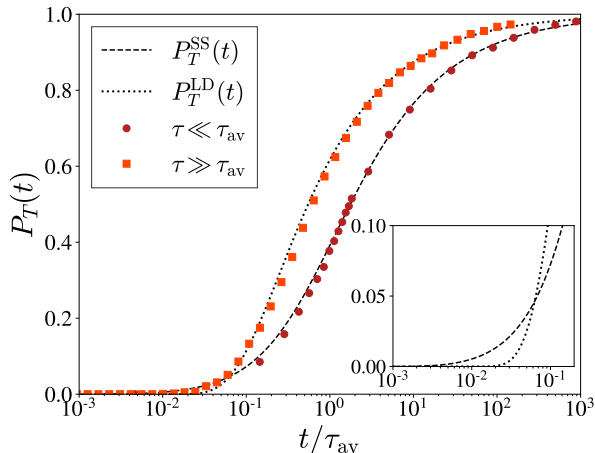


Figure 3. Gaussian and non-Gaussian targeting for the GCP at  $p = 0.99$ . Dashed and dotted lines reproduce  $P_T^{\text{SS}}(t)$  and  $P_T^{\text{LD}}(t)$ , respectively. The time axis is rescaled by  $\tau_{\text{av}}$  defined in Eq. (37) so that the plot is independent of  $x_0$ . Colored filled symbols are obtained simulating the birth-death polymerization process and the consequent polymer diffusion with the appropriate, time-varying diffusion coefficient; values for  $\mu$  in Eq. (18) has been chosen to satisfy the limits reported in the legend. Inset: magnification of  $P_T^{\text{SS}}(t)$  and  $P_T^{\text{LD}}(t)$  for small time.

highlight the two regimes for the GCP model with the semi-infinite domain; a similar plot is valid for the DD model [24]. The abscissa is rescaled by the characteristic time for the particle with an average diffusion coefficient to travel over the distance from the target, namely

$$\tau_{\text{av}} \equiv \frac{x_0^2}{2 D_{\text{av}}}. \quad (37)$$

As shown above,  $\tau_T(x_0, D)$  is a convex function of  $D$ . Taking now  $\varphi(D) \equiv \tau_T(x_0, D)$ , and again  $f(D) = D$ , the Jensen's inequality[37] conveys the following basic result:

$$\tau_T^{\text{SS}}(x_0) \equiv \mathbb{E}[\tau_T(x_0, D)] > \tau_T^{\text{LD}}(x_0) \equiv \tau_T(x_0, D_{\text{av}}). \quad (38)$$

Since Jensen's inequality is valid when averaging on general distributions, Eq. (38) applies to the DD and the GPC models, and also for CTRWs if we compare the early behavior ruled by the discrete subordination formula, Eq. (19), with the LD Gaussian limit, attained for  $t \gg \tau$ . We thus conclude, consistently with earlier specific findings [22–24], that *for a single searcher within the general class of non-Gaussian diffusion processes based on subordination, the characteristic time to target is larger than in ordinary diffusion*. As the characteristic time to target in ordinary diffusion is in general inversely related to  $D$ , this finding extends to general transient regimes and targeting processes, not necessarily one-dimensional. It is an effect due to the excess of probability in the central part of the PDF (slower diffusers) (see Fig. 1) and it is somehow at odds with the

general prospect of surprising phenomena triggered by rare fluctuations [2].

What about the “tail effect” in Fig. 1? By inspecting  $P_T^{\text{SS}}(t|x_0)$  and  $P_T^{\text{LD}}(t|x_0)$ , one finds that typically the latter is larger than the former, consistently with Eq. (38). However, a closer look reveals that the “tail effect” dominates at time shorter than  $\tau_T^*$  (Fig. 3, inset), with  $\tau_T^*$  being the solution of

$$\sum_{n=1}^{\infty} p_D^*(D_n) P_T(\tau_T^*|x_0, D_n) = P_T(\tau_T^*|x_0, D_{\text{av}}). \quad (39)$$

The corresponding fraction  $P_T(\tau_T^*|x_0, D_{\text{av}})$  of successful single-particle searches below which non-Gaussian chases are more efficient than the BG ones is typically small; for instance  $\tau_T^* \simeq 6.3 \times 10^{-2} \tau_{\text{av}}$  and  $P_T(\tau_T^*|x_0, D_{\text{av}}) \simeq 4.6 \times 10^{-2}$  in Fig. 3. However, this apparently negligible effect makes a drastic difference in *extreme* first passage problems, where a small fraction of the total number of searchers is required to first reach the target to activate a certain function. This finding is discussed in details in the companion paper, Ref. [38].

## CONCLUSIONS

Targeting of receptors by ligand particles is a fundamental biological mechanism used by cells to activate or stop specific functions. The mechanism makes use of the diffusive properties of the ligands and the basic quantity to measure is the characteristic time employed by a searcher to reach the target, i.e., when it exists finite, the mean first passage time. Since recent experiments and simulations highlighted heterogeneous conditions in which diffusion becomes Brownian non-Gaussian, the question arose whether non-Gaussianity enhances or not searches.

While this issue has already been addressed for specific models [22–24], here we have provided a general approach valid for all Brownian non-Gaussian processes based on subordination. Using Jensen's inequality and the positiveness of the variance of the subordinator, we have demonstrated that the distributions of subordinated diffusive particles display an excess of probability both in the central part and in the tails, when compared with Gaussians. The qualitative features appearing in Fig. 1 are independent of the kind of subordinator. At variance, the dynamical regimes shown in Fig. 2 depend on the specific definition of the subordinator. The DD and GCP models display both the SS and the LD regimes. The FSP model is characterized by the SS regime only, and the CTRW model with exponential waiting times possesses exclusively the LD regime.

In agreement with earlier findings, we have shown on general ground that the “central effect” dominates the one-particle searching process, making the characteristic time to target larger than in ordinary Gaussian

diffusion. This conclusion encompasses current models of Brownian non-Gaussian diffusion and implies that, for ordinary diffusion-limited-reaction scenarios, non-Gaussianity weakens reaction rates.

The “tail effect” pertains to the realm of rare events and control instead, *extreme* searches, where only a few among many diffusers are required to reach the target. In Ref. [38] it is shown that this is the context in which non-Gaussianity makes a substantial difference.

## ACKNOWLEDGMENTS

F.S. and F.B. acknowledge the support by the project MUR-PRIN 2022ETXBEY, “Fickian non-Gaussian diffusion in static and dynamic environments”, funded by the European Union – Next Generation EU”. V.S. acknowledges the support from the European Commission through the Marie Skłodowska-Curie COFUND project REWIRE, grant agreement No. 847693. A.C. acknowledges the support of the Polish National Agency for Academic Exchange (NAWA).

---

\* vittoria.sposini@univie.ac.at

† sparampo@gitam.edu

‡ chechkin@uni-potsdam.de

§ enzo.orlandini@unipd.it

¶ flavio.seno@unipd.it

\*\* fulvio.baldovin@unipd.it

- [1] B. Wang, S. M. Anthony, S. C. Bae, and S. Granick, *Proceedings of the National Academy of Sciences* **106**, 15160 (2009).
- [2] B. Wang, J. Kuo, S. C. Bae, and S. Granick, *Nature materials* **11**, 481 (2012).
- [3] T. Toyota, D. A. Head, C. F. Schmidt, and D. Mizuno, *Soft Matter* **7**, 3234 (2011).
- [4] C. Yu, J. Guan, K. Chen, S. C. Bae, and S. Granick, *ACS Nano* **7**, 9735 (2013).
- [5] C. Yu and S. Granick, *Langmuir* **30**, 14538 (2014).
- [6] I. Chakraborty and Y. Roichman, *Physical Review Research* **2**, 022020 (2020).
- [7] E. R. Weeks, J. C. Crocker, A. C. Levitt, A. Schofield, and D. A. Weitz, *Science* **287**, 627 (2000).
- [8] C. E. Wagner, B. S. Turner, M. Rubinstein, G. H. McKinley, and K. Ribbeck, *Biomacromolecules* **18**, 3654 (2017).
- [9] J.-H. Jeon, M. Javanainen, H. Martinez-Seara, R. Metzler, and I. Vattulainen, *Physical Review X* **6**, 021006 (2016).
- [10] E. Yamamoto, T. Akimoto, A. C. Kalli, K. Yasuoka, and M. S. Sansom, *Science advances* **3**, e1601871 (2017).
- [11] S. Stylianidou, N. J. Kuwada, and P. A. Wiggins, *Biophysical journal* **107**, 2684 (2014).
- [12] B. R. Parry, I. V. Surovtsev, M. T. Cabeen, C. S. O’Hern, E. R. Dufresne, and C. Jacobs-Wagner, *Cell* **156**, 183 (2014).
- [13] M. C. Munder, D. Midtvedt, T. Franzmann, E. Nuske, O. Otto, M. Herbig, E. Ulbricht, P. Müller, A. Taubenberger, S. Maharana, *et al.*, *elife* **5**, e09347 (2016).
- [14] A. G. Cherstvy, O. Nagel, C. Beta, and R. Metzler, *Physical Chemistry Chemical Physics* **20**, 23034 (2018).
- [15] Y. Li, F. Marchesoni, D. Debnath, and P. K. Ghosh, *Physical Review Research* **1**, 033003 (2019).
- [16] A. Cuetos, N. Morillo, and A. Patti, *Physical Review E* **98**, 042129 (2018).
- [17] S. Hapca, J. W. Crawford, and I. M. Young, *Journal of the Royal Society Interface* **6**, 111 (2009).
- [18] R. Pastore, A. Ciarlo, G. Pesce, F. Greco, and A. Sasso, *Physical Review Letters* **126**, 158003 (2021).
- [19] R. Pastore and G. Raos, *Soft Matter* **11**, 8083 (2015).
- [20] J. M. Miotto, S. Pigolotti, A. V. Chechkin, and S. Roldán-Vargas, *Physical Review X* **11**, 031002 (2021).
- [21] F. Rusciano, R. Pastore, and F. Greco, *Physical Review Letters* **128**, 168001 (2022).
- [22] Y. Lanoiselée, N. Moutal, and D. S. Grebenkov, *Nat. Comm.* **9**, 4398 (2018).
- [23] D. S. Grebenkov, *J. Phys. A* **52**, 174001 (2019).
- [24] V. Sposini, A. Chechkin, and R. Metzler, *Journal of Physics A: Mathematical and Theoretical* **52**, 04LT01 (2019).
- [25] A. V. Chechkin, F. Seno, R. Metzler, and I. M. Sokolov, *Physical Review X* **7**, 021002 (2017).
- [26] S. Nampoothiri, E. Orlandini, F. Seno, and F. Baldovin, *Physical Review E* **104**, L062501 (2021).
- [27] S. Nampoothiri, E. Orlandini, F. Seno, and F. Baldovin, *New J. Phys.* **24**, 023003 (2022).
- [28] B. Marcone, S. Nampoothiri, E. Orlandini, F. Seno, and F. Baldovin, *J. Phys. A: Math. Theor.* **55**, 354003 (2022).
- [29] P. Flory, *Principles of Polymer Chemistry* (Cornell University Press, 1953).
- [30] T. Cosgrove, *Colloid Science Principles, Methods and Applications* (Blackwell Publishing, Oxford, UK, 2005).
- [31] G. Odian, *Principles of Polymerization* (John Wiley & Sons, 2004).
- [32] J. Klafter and I. Sokolov, *First Steps in Random Walks: From Tools to Applications* (Oxford University Press, 2011).
- [33] E. Barkai and S. Burov, *Physical Review Letters* **124**, 060603 (2020).
- [34] W. Wang, E. Barkai, and S. Burov, *Entropy* **22**, 697 (2020).
- [35] A. Pacheco-Pozo and I. M. Sokolov, *Physical Review Letters* **127**, 120601 (2021).
- [36] A. Pacheco-Pozo and I. M. Sokolov, *Physical Review E* **103**, 042116 (2021).
- [37] W. Rudin, *Real and complex analysis* (McGraw-Hill, 1987).
- [38] V. Sposini, S. Nampoothiri, A. Chechkin, E. Orlandini, F. Seno, and F. Baldovin, *Physical Review Letters* **132**, 117101 (2024).
- [39] W. Feller, *An Introduction to Probability Theory and Its Applications* (John Wiley & Sons, 1968).
- [40] S. Bochner, *Harmonic analysis and the theory of probability* (University of California press, 2020).
- [41] S. Heston, *Rev. Financial Studies* **6**, 327 (1993).
- [42] J.-P. Fouqué, G. Papanicolaou, and K. Sircar, *Derivatives in Financial Markets with Stochastic Volatility* (Cambridge University Press, Cambridge, England, 2000).
- [43] P.-G. de Gennes, *Scaling Concepts in Polymer Physics* (Cornell University Press, 1979).

- [44] M. Doi and E. S. F., *The Theory of Polymer Dynamics* (Oxford University Press, 1992).
- [45] D. T. Gillespie, *Journal of Physical Chemistry* **81**, 2340–2361 (1977).
- [46] C. Beck and E. G. Cohen, *Physica A: Statistical mechanics and its applications* **322**, 267 (2003).
- [47] C. Beck, *Progress of Theoretical Physics Supplement* **162**, 29 (2006).
- [48] H. Touchette, *Physics Reports* **478**, 1 (2009).
- [49] S. Redner, *A guide to first passage processes* (Cambridge University Press, 2001).